Supporting Information

Selective Electrocatalytic Hydrogenation of Phenol to Value-added Products Using PtRu Electrodes: Closing Carbon Balance by Capturing Gas-Phase Cyclohexane

Xiaolong Lu [a,1], Hongjie Guo [a,1], Yu Li [a], Fuqiang Liu [b], Qizheng Zhuo [c], Shuai Yang [a], Xiaohong Guan [b], Changyong Zhang [*,a]

[a] State Key Laboratory of Advanced Environmental Technology, Department of Environmental Science and Engineering, University of Science and Technology of China, Hefei 230026, China

[b] Shanghai Engineering Research Center of Biotransformation of Organic Solid Waste, School of Ecological and Environmental Sciences, East China Normal University, Shanghai 200241, China

[c] College of Environmental and Resource Sciences, Zhejiang University, Hangzhou 320058, China

ENGINEERING Environment

Number of Pages: 16

Number of Figures: 12

Number of Tables: 1

Number of Texts: 1

* Corresponding authors.
E-mail address: changyongzhang@ustc.edu.cn (C. Zhang)

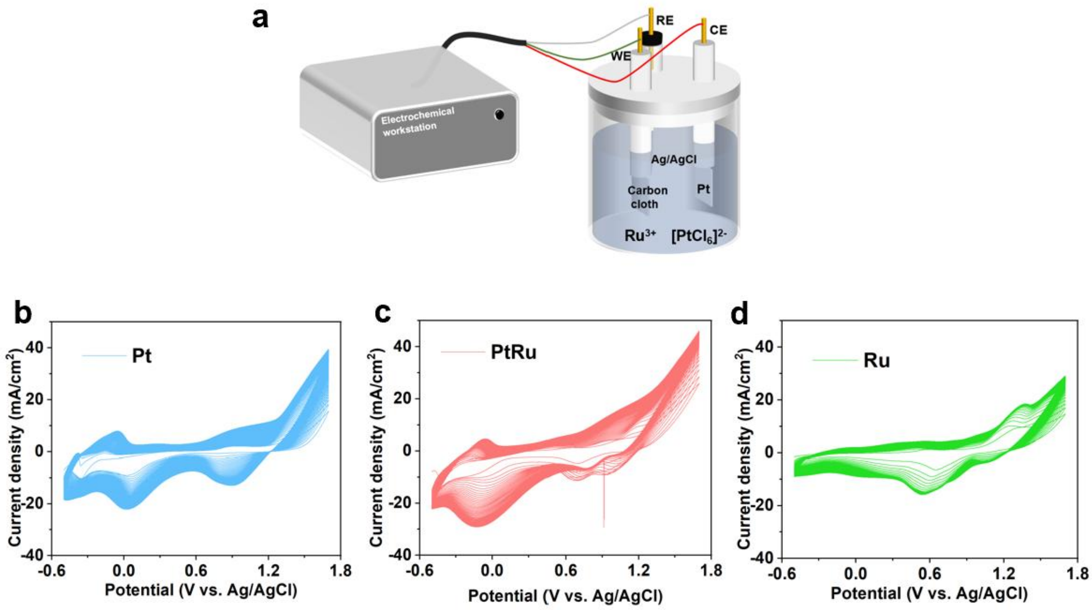

Fig. S1. (a) Schematic illustration of the preparation process of electrode by cyclic electrodeposition method. (b-d) CV curves of electrodeposition processes for Pt, PtRu, Ru.

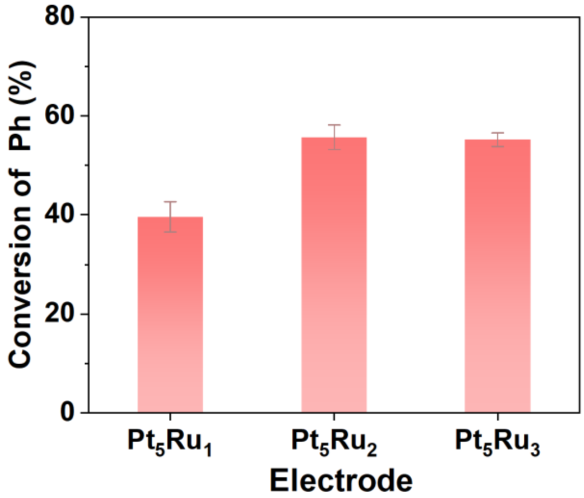

Fig. S2. Optimization of electrodeposition molar ratio of Pt/Ru. Reaction conditions: 40 mL of 0.1 M H_2SO_4 with 25 mM Ph, −0.40 V vs Ag/AgCl, 60 min.

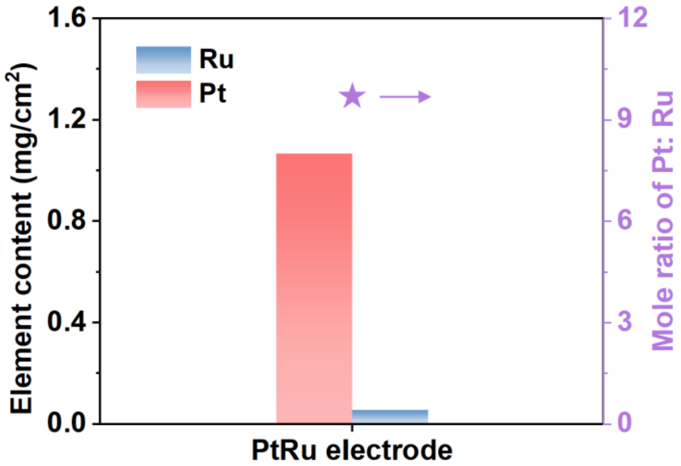

Fig. S3. Pt and Ru contents of PtRu electrode by ICP-AES.

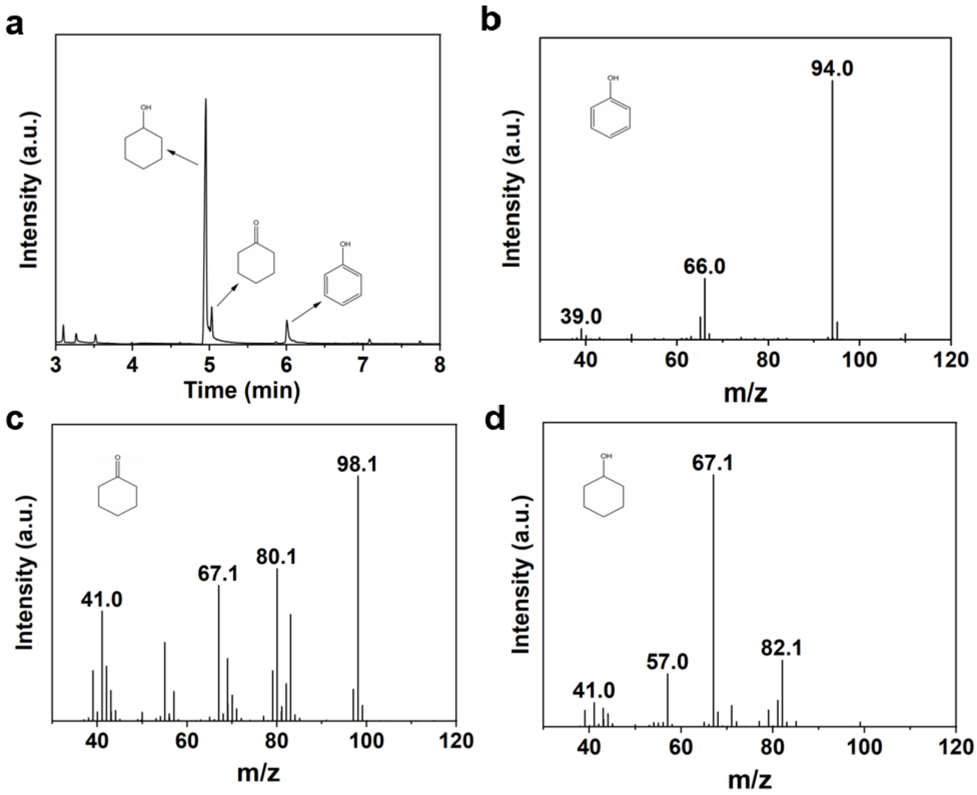

Fig. S4. The identification of the products by GC-MS analysis.

Table S1. Summary of reported carbon balance in phenol ECH on Pt-based catalysts.

Catalyst	Electrolyte	Selectivity (%)		Carbon balance (%)	Reference
		Cyclohexanone	Cyclohexanol		
Pt/SSB	0.1 M Na_2SO_4	55	20	75	(Lu et al., 2023)
Pt/SBA-15	0.1 M Na_2SO_4	50	40	90	(Lu et al., 2023)
Pt/CB	0.1 M Na_2SO_4	30	45	75	(Lu et al., 2023)
Pt/C-com	0.1 M $HClO_4$	50	30	80	(Liu et al., 2024b)
Pt/TiO_2	0.1 M $HClO_4$	75	5	80	(Liu et al., 2024b)
Pt	0.2 M $HClO_4$	50	30	80	(Liu et al., 2024a)
PtRu	0.1 M H_2SO_4	3	60	63	This work

Note: After the gas absorption device was employed, the formation of cyclohexane was detected in this work, with the carbon balance rate reaching over 95%.

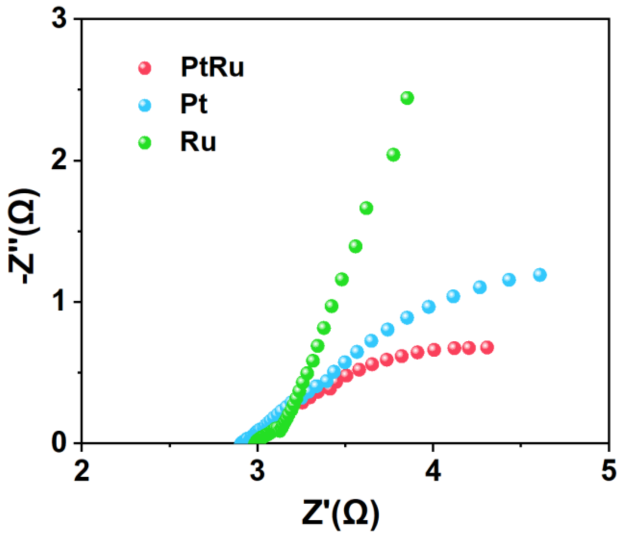

Fig. S5. Nyquist plots of different electrodes in 0.1 M H_2SO_4 with 25 mM phenol.

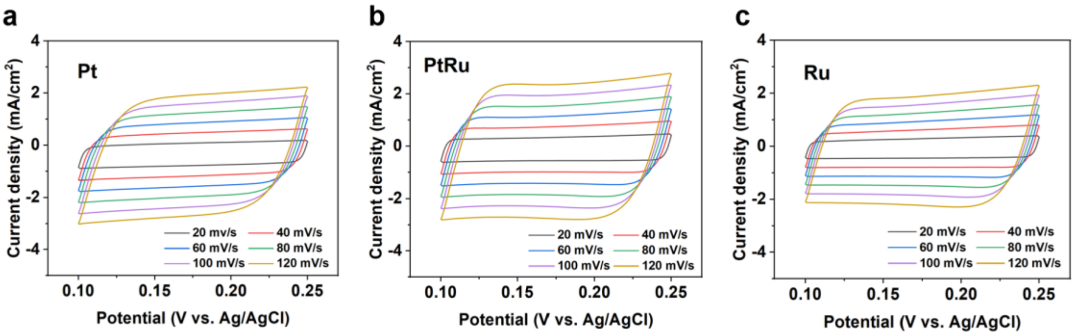

Fig. S6. CV curves at various scan rates of (a) Pt, (b) PtRu, (c) Ru in 0.1 M H_2SO_4.

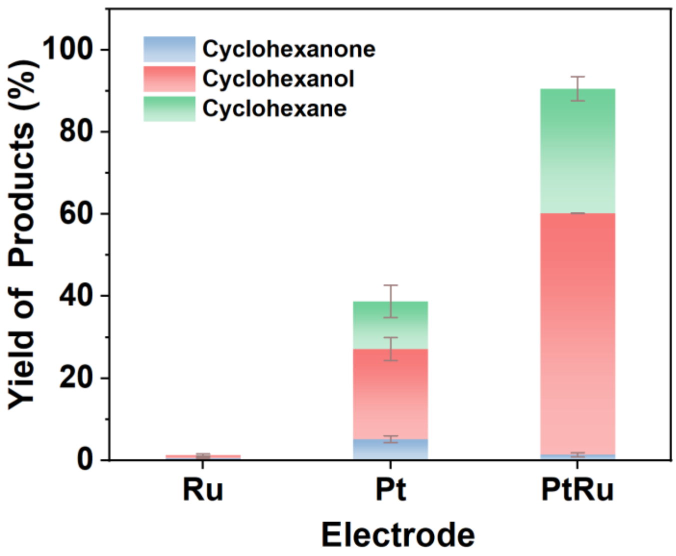

Fig. S7. Yield of products by using different electrodes. Reaction conditions: 40 mL of 0.1 M H_2SO_4 with 25 mM Ph, −0.40 V vs Ag/AgCl, 120 min.

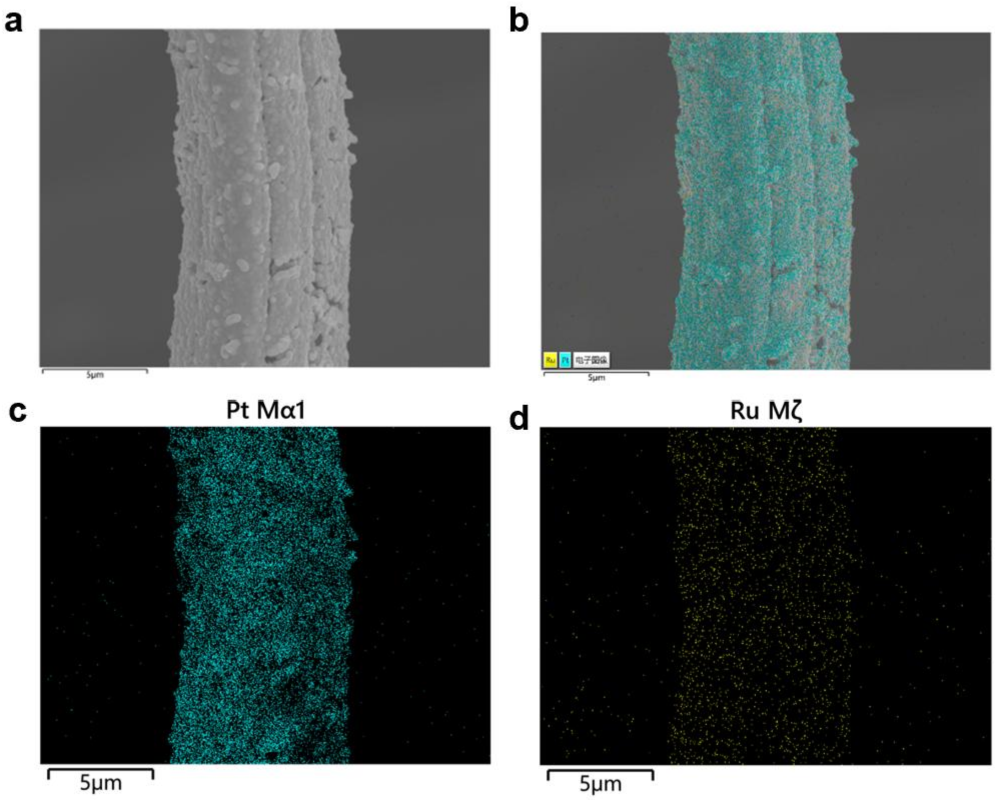

Fig. S8. SEM-elemental mapping images of PtRu after electrolysis

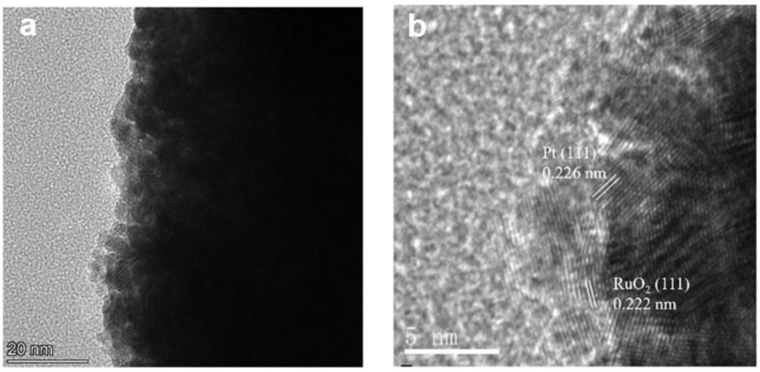

Fig. S9. TEM images of PtRu after electrolysis

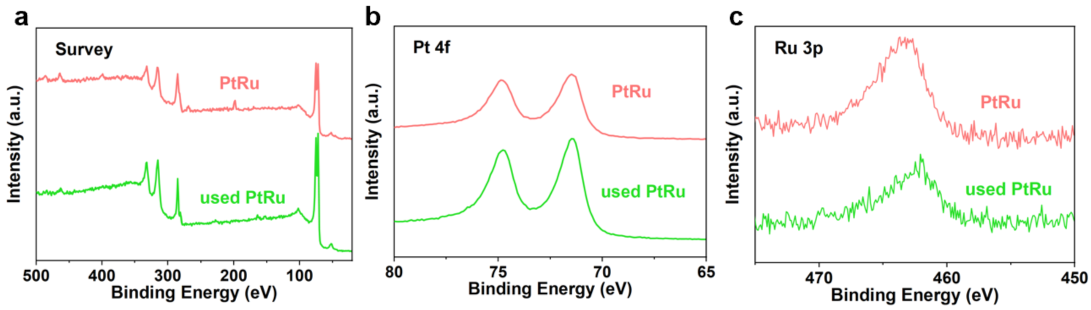

Fig. S10. XPS spectra of PtRu electrode before and after electrolysis: (a) survey spectrum, (b-c) corresponding high resolution XPS spectra of Pt 4f and Ru 3p.

Text S1. Density Functional Theory (DFT) calculations

All density functional theory (DFT) calculations were performed by Vienna ab initio simulation package (VASP) (Kresse and Furthmüller, 1996) using the projector augmented wave (PAW) potentials with a planewave cutoff energy of 500 eV (Kresse and Joubert, 1999). The generalized gradient approximation (GGA) functional of Perdew, Burke, and Ernzerhof (PBE) was applied as the exchange-correlation functional (Perdew et al., 1996). The (111) slab of Pt metal and PtRu alloy were constructed with four layers. A vacuum region of 20 Å was added to the surface to eliminate the effects between two adjacent layers. During the calculation, the bottom two layers were fixed. The convergence criteria of electronic energies and atomic forces for all calculations were 10^{-5} eV and 0.02 eV/Å.

The calculated adsorption energy (E_{ads}) was evaluated based on the following equation:

$$\Delta E_{ads} = E_{sur+adsorbate} - E_{sur} - E_{adsorbate} \quad (1)$$

where $E_{sur+adsorbate}$, E_{sur}, and $E_{adsorbate}$ are the obtained energies for the slab system containing the adsorbate, the energy of the slab, and the energy of the adsorbate in a vacuum, respectively.

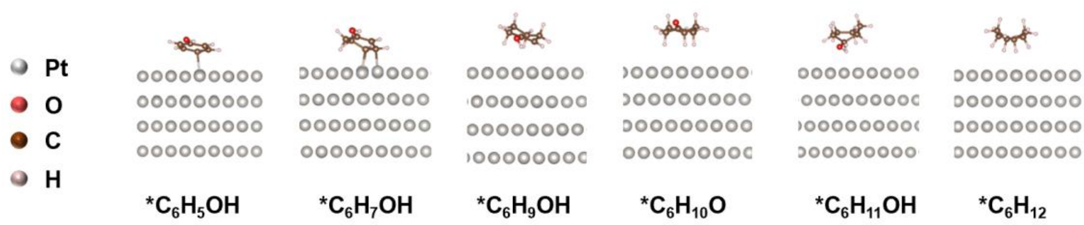

Fig. S11. Optimized configurations of the ECH of phenol process on Pt (111).

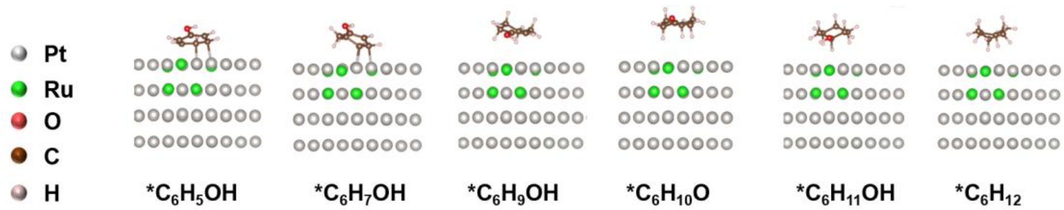

Fig. S12. Optimized configurations of the ECH of phenol process on PtRu (111).

Reference

Kresse G, Furthmüller J (1996). Efficient iterative schemes for ab initio total-energy calculations using a plane-wave basis set. Physical Review B, 54(16): 11169-11186

Kresse G, Joubert D (1999). From ultrasoft pseudopotentials to the projector augmented-wave method. Physical Review B, 59(3): 1758-1775

Liu F, Gao X, Guo Z, Tse E C M, Chen Y (2024a). Sustainable Adipic Acid Production via Paired Electrolysis of Lignin-Derived Phenolic Compounds with Water as Hydrogen and Oxygen Sources. Journal of the American Chemical Society, 146(22): 15275-15285

Liu Y, Ji K, Wang X, Shi Q, Li A Z, Yin Z, Zhu Y Q, Duan H (2024b). Modulating the Coverage of Adsorbed Hydrogen via Hydrogen Spillover Enables Selective Electrocatalytic Hydrogenation of Phenol to Cyclohexanone. Angewandte Chemie International Edition, 64(7)

Lu X, Wang J, Peng W, Li N, Liang L, Cheng Z, Yan B, Yang G, Chen G (2023). Electrocatalytic hydrogenation of phenol by active sites on Pt-decorated shrimp shell biochar catalysts: Performance and internal mechanism. Fuel, 331

Perdew J P, Burke K, Ernzerhof M (1996). Generalized Gradient Approximation Made Simple. Physical Review Letters, 77(18): 3865-3868